12

THE SPIN–BOSON MODEL

Sometimes, you know, we can not see dazzling objects
Through an excess of light; whoever heard
Of doorways, portals, outlooks, in such trouble?
Besides, if eyes are doorways, might it not
Be better to remove them, sash, jamb, lintel,
And let the spirit have a wider field?

Lucretius (c.99–c.55 BCE*) "The way things are"*
translated by Rolfe Humphries, Indiana University Press, 1968

In a generic quantum mechanical description of a molecule interacting with its thermal environment, the molecule is represented as a few level system (in the simplest description just two, for example, ground and excited states) and the environment is often modeled as a bath of harmonic oscillators (see Section 6.5). The resulting theoretical framework is known as *the spin–boson model*,[1] a term that seems to have emerged in the Kondo problem literature (which deals with the behavior of magnetic impurities in metals) during the 1960s, but is now used in a much broader context. Indeed, it has become one of the central models of theoretical physics, with applications in physics, chemistry, and biology that range far beyond the subject of this book. Transitions between molecular electronic states coupled

---

[1] The term "spin–boson model" seems to have emerged in the Kondo problem literature (which deals with the interactions between an impurity spin in a metal and the surrounding electron bath) during the 1960s, however fundamental works that use different aspects of this model were published earlier. In 1953, Wangsness and Bloch (R. K. Wangsness and F. Bloch, Phys. Rev. **89**, 728 (1953)) presented a framework for the theoretical discussion of spin relaxation due to environmental interactions, that evolved into theory of the Bloch equations in a later paper by Bloch (F. Bloch, Phys. Rev. **105**, 1206 (1957)) and the more rigorous description by Redfield (A. G. Redfield, IBM J. Res. Develop. **1**, 19 (1957)); see Section 10.4.8. Marcus (R. A. Marcus, J. Chem. Phys. **24**, 966; 979 (1956); see Chapter 16) has laid the foundation of the theory of electron transfer in polar solvents and Holstein (T. Holstein, Ann. Phys. (NY), **8**, 325; 343 (1959)) published his treatise of polaron formation and dynamics in polar crystals. Much of the later condensed phase literature has been reviewed by Leggett et al. (A. J. Leggett, S. Chakravarty, A. T. Dorsey, M. P. A. Fisher, A. Garg, W. Zwerger, Rev. Mod. Phys. **59**, 1 (1987)), see also H. Grabert and A. Nitzan, editors, Chem. Phys. **296**(2–3) (2004). In many ways the problem of a few level system interacting with the radiation field (Chapter 18) also belong to this class of problems.

---

to nuclear vibrations, environmental phonons, and photon modes of the radiation field fall within this class of problems. The present chapter discusses this model and some of its mathematical implications. The reader may note that some of the subjects discussed in Chapter 9 are reiterated here in this more general framework.

12.1 Introduction

In Sections 2.2 and 2.9 we have discussed the dynamics of the two-level system and of the harmonic oscillator, respectively. These exactly soluble models are often used as prototypes of important classes of physical system. The harmonic oscillator is an exact model for a mode of the radiation field (Chapter 3) and provides good starting points for describing nuclear motions in molecules and in solid environments (Chapter 4). It can also describe the short-time dynamics of liquid environments via the instantaneous normal mode approach (see Section 6.5.4). In fact, many linear response treatments in both classical and quantum dynamics lead to harmonic oscillator models: Linear response implies that forces responsible for the return of a system to equilibrium depend linearly on the deviation from equilibrium—a harmonic oscillator property! We will see a specific example of this phenomenology in our discussion of dielectric response in Section 16.9.

The two-level model is the simplest prototype of a quantum mechanical system that has no classical analog. A spin $\frac{1}{2}$ particle is of course an example, but the same model is often used also to describe processes in multilevel systems when the dynamics is dominated by two of the levels. The dynamics of an anharmonic oscillator at low enough temperatures may be dominated by just the two lowest energy levels. The electronic response of a molecular system is often dominated by just the ground and the first excited electronic states. Low temperature tunneling dynamics in a double well potential can be described in terms of an interacting two-level system, each level being the ground state on one of the wells when it is isolated from the other. Finally, as a mathematical model, the two-level dynamics is often a good starting point for understanding the dynamics of a few level systems.

The prominence of these quantum dynamical models is also exemplified by the abundance of theoretical pictures based on the spin–boson model—a two (more generally a few) level system coupled to one or many harmonic oscillators. Simple examples are an atom (well characterized at room temperature by its ground and first excited states, that is, a two-level system) interacting with the radiation field (a collection of harmonic modes) or an electron spin interacting with the phonon modes of a surrounding lattice, however this model has found many other applications in a variety of physical and chemical phenomena (and their extensions into the biological world) such as atoms and molecules interacting with the radiation field, polaron formation and dynamics in condensed environments,

electron transfer processes, quantum solvation phenomena, spin–lattice relaxation, molecular vibrational relaxation, exciton dynamics in solids, impurity relaxation in solids, interaction of magnetic moments with their magnetic environment, quantum computing (the need to understand and possibly control relaxation effects in quantum bits, or qubits), and more. In addition, the spin–boson model has been extensively used as a playground for developing, exploring, and testing new theoretical methods, approximations, and numerical schemes for quantum relaxation processes, including perturbation methods, exactly solvable models, quantum-numerical methodologies and semiclassical approximations. A few of these results and applications are presented below.

12.2 The model

We consider a two-level system coupled to a bath of harmonic oscillators that will be referred to as a *boson field*. Two variations of this model, which differ from each other by the basis used to describe the two-level system, are frequently encountered. In one, the basis is made of the eigenstates of the two-state Hamiltonian that describes the isolated system. The full Hamiltonian is then written

$$\hat{H} = \hat{H}_0 + \hat{V}_{\mathrm{SB}} \tag{12.1}$$

where the zero-order Hamiltonian describes the separated subsystems (see Fig. 12.1)

$$\hat{H}_0 = \hat{H}_M + \hat{H}_B = E_1|1\rangle\langle 1| + E_2|2\rangle\langle 2| + \sum_\alpha \hbar\omega_\alpha \hat{a}_\alpha^\dagger \hat{a}_\alpha \tag{12.2a}$$

and the coupling is taken in the form

$$\hat{V}_{\mathrm{SB}} = \sum_{j,j'=1}^{2} \sum_\alpha V_{j,j'}^\alpha |j\rangle\langle j'|(\hat{a}_\alpha^\dagger + \hat{a}_\alpha) \tag{12.2b}$$

The rationale behind this choice of system–bath interaction is that it represents the first term in the expansion of a general interaction between the
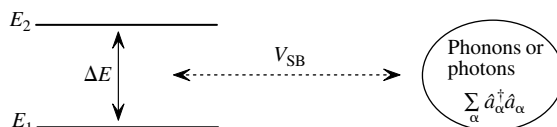

FIG. 12.1 The spin–boson model for a two-level molecule coupled to a system of harmonic oscillators.

two-level system and the harmonic bath in the bath normal mode coordinates, $\hat{x}_\alpha = \sqrt{\hbar/(2m_\alpha\omega_\alpha)}(\hat{a}_\alpha^\dagger + \hat{a}_\alpha)$, that express deviations from the minimum energy configuration.[2] In other situations the coupling takes place through the momentum operator which is linear in $(\hat{a}_\alpha^\dagger - \hat{a}_\alpha)$. An example is the important case of system–radiation field coupling. If the system does not have a permanent dipole moment the coupling $\hat{V}_{SB}$ is non-diagonal in the system states and takes the form (cf. Eq. (3.27))

$$\hat{V}_{SB} = -i\sum_{\mathbf{k}}\sum_{\sigma_{\mathbf{k}}}\sqrt{\frac{2\pi\hbar\omega_k}{\varepsilon\Omega}}[(\hat{\mu}_{12}\cdot\sigma_{\mathbf{k}})|1\rangle\langle 2| + (\hat{\mu}_{21}\cdot\sigma_{\mathbf{k}})|2\rangle\langle 1|](\hat{a}_{\mathbf{k},\sigma_{\mathbf{k}}} - \hat{a}_{\mathbf{k},\sigma_{\mathbf{k}}}^\dagger)$$

$$(12.3)$$

where $\hat{\mu}$ is the system dipole operator and where the harmonic modes are characterized in terms of the wavevector $\mathbf{k}$ and the polarization vector $\sigma_{\mathbf{k}}$.

In the second model, the basis chosen to describe the two-level (or few level) system is not made of the system eigenstates. In what follows we denote these states $|L\rangle$ and $|R\rangle$

$$\hat{H} = \hat{H}_0 + \hat{V}_S + \hat{V}_{SB} \tag{12.4}$$

$\hat{H}_0$ and $\hat{V}_{SB}$ have the forms (12.2)

$$\hat{H}_0 = \hat{H}_{0M} + \hat{H}_{0B} = E_L|L\rangle\langle L| + E_R|R\rangle\langle R| + \sum_\alpha \hbar\omega_\alpha \hat{a}_\alpha^\dagger \hat{a}_\alpha \tag{12.5a}$$

$$\hat{V}_{SB} = \sum_{j,j'=L}^{R}\sum_\alpha V_{j,j'}^\alpha |j\rangle\langle j'|(\hat{a}_\alpha^\dagger + \hat{a}_\alpha) \tag{12.5b}$$

and the additional term is the non-diagonal part of the system Hamiltonian

$$\hat{V}_S = V_{LR}^S|L\rangle\langle R| + V_{RL}^S|R\rangle\langle L| \tag{12.6}$$

Sometimes this is done as a computational strategy, for example, atomic orbitals are used as a basis set in most molecular computations. In other cases this choice reflects our physical insight. Consider, for example, tunneling in a double well potential U, Fig. 12.2(a), where the barrier between the two wells is high relative to both the thermal energy k_BT and the zero-point energy in each well. We have already indicated that a two-level model can be useful for describing the low-temperature dynamics of this system. Denoting by ψ_L and ψ_R the wavefunctions that represent the ground states of the separated potentials U_L, Fig. 12.2(b), and U_R, Fig. 12.2(c),

---

[2] The zero-order term of this expansion, which is independent of x_α, just redefines the zero-order Hamiltonian. Disregarding higher order reflects the expectation that in condensed phases the deviations x_α from the minimum energy configuration are small.
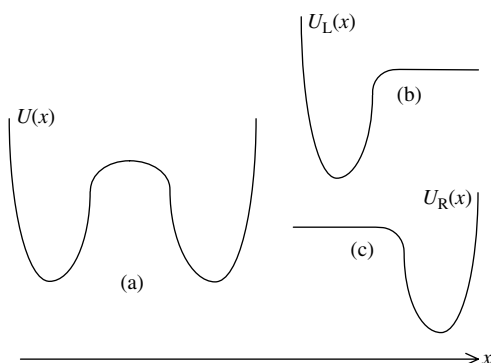
FIG. 12.2 A double well potential $U(x)$ (a) and the potentials $U_L(x)$ and $U_R(x)$, (b) and (c), which define the states $|L\rangle$ and $|R\rangle$ used in the local state representation of a 2-level system.

respectively, the two lowest states of the potential U are approximated well by the even and odd linear combinations, $\psi_{1,2} = \psi_L \pm \psi_R$. While $\psi_{1,2}$ represent the exact ground states of the potential $U(x)$, tunneling is more readily described in terms of transitions between the local states ψ_R and ψ_L.

It should be emphasized that, while the two models, Eqs (12.1), (12.2) and (12.4)–(12.6) are mathematically just different representations of what may be seen as the same Hamiltonian, they are used in different physical contexts. The former model is used to describe transitions between system eigenstates that are induced by the interaction of a two-level system with a boson field, as exemplified by the interaction between a system and a radiation field, Eq. (12.3). In contrast, the latter model is used to examine the effect of a boson bath on the transition between states of the system that are (1) coupled to each other also in the absence of this field and (2) associated with distinctly different polarizations of the boson environment in the different system states. This is exemplified by the electron transfer problem discussed in Chapter 16, where states L and R correspond to charge localization at different spatial positions in a polar solvent. Obviously, a two-level system may be described in terms of its eigenstates or any other basis, and the dynamics caused by its coupling to an external field or a thermal bath can be studied in any representation. Physical reality often guides us to choose a particular representation. In the tunneling example discussed above and in the electron transfer problem of Chapter 16 the local state representation is convenient because the system can be initially prepared such a local state. We have encountered a similar example in Chapter 9, where the study of the decay of a prepared "doorway" state coupled to a continuous manifold of background states was studied in the representation defined by these states and not by the eigenstates of the system Hamiltonian, because such a doorway state could be experimentally prepared and monitored.

Choosing a physically motivated representation is useful in developing physically guided approximation schemes. A commonly used approximation for the model (12.4)–(12.6) is to disregard terms with $j \neq j'$ in the system–bath interaction (12.5b). The overall Hamiltonian then takes the form

$$\hat{H} = \left[E_L + \sum_\alpha V_L^\alpha (\hat{a}_\alpha^\dagger + \hat{a}_\alpha) \right] |L\rangle\langle L| + \left[E_R + \sum_\alpha V_R^\alpha (\hat{a}_\alpha^\dagger + \hat{a}_\alpha) \right] |R\rangle\langle R|$$

$$+ V_{LR}|L\rangle\langle R| + V_{RL}|R\rangle\langle L| + \sum_\alpha \hbar\omega_\alpha \hat{a}_\alpha^\dagger \hat{a}_\alpha \qquad (12.7)$$

The spin–boson coupling in this Hamiltonian is diagonal in the local state basis. The rationale for this model is that in this local state representation bath induced coupling between different local states is small relative to the interstates coupling V_{RL} because the corresponding local wavefunctions almost do not overlap. However the bath affects the system in states L and R in a substantial way. Its effect in the Hamiltonian (12.7) appears as fluctuations in the local state energies associated with the instantaneous configurations of the harmonic bath (again expanded to first order in the bath coordinates). Interestingly, the Hamiltonian (12.7) can be transformed to a form similar to (12.3) but with a nonlinear coupling to the boson field. This is shown in the next section.

12.3   The polaron transformation

Consider the n-level equivalent of the Hamiltonian (12.7)

$$\hat{H} = \sum_n \left(E_n + \sum_\alpha g_{n\alpha} \hat{x}_\alpha \right) |n\rangle\langle n| + \sum_{n \neq n'} V_{n,n'} |n\rangle\langle n'| + \hat{H}_B(\{\hat{p}_\alpha, \hat{x}_\alpha\}) \qquad (12.8)$$

where (using (2.153))

$$g_{n\alpha} = V_n^\alpha \sqrt{\frac{2m_\alpha \omega_\alpha}{\hbar}} \qquad (12.9)$$

and where

$$H_B(\{\hat{p}_\alpha, \hat{x}_\alpha\}) = \sum_\alpha \left(\frac{\hat{p}_\alpha^2}{2m_\alpha} + \frac{1}{2} m_\alpha \omega_a^2 \hat{x}_\alpha^2 \right) \qquad (12.10)$$

is the harmonic bath Hamiltonian, with $\hat{x}_\alpha$, $\hat{p}_\alpha$, ω_a, and m_α denoting the position and momentum operators, the frequency and mass, respectively, of the harmonic

bath modes. We now carry the unitary transformation, known as the *polaron transformation*

$$\hat{\bar{H}} = \hat{U}\hat{H}\hat{U}^{-1}; \qquad \hat{U} \equiv \prod_n \hat{U}_n \tag{12.11a}$$

$$\hat{U}_n = \exp(-i|n\rangle\langle n|\hat{\Omega}_n); \qquad \hat{\Omega}_n = \sum_\alpha \hat{\Omega}_{n,\alpha} \tag{12.11b}$$

$$\hat{\Omega}_{n,\alpha} = \frac{g_{n\alpha}\hat{p}_\alpha}{\hbar m_\alpha \omega_\alpha^2} \Rightarrow i\hat{\Omega}_{n,\alpha} = \frac{g_{n\alpha}}{m_\alpha \omega_\alpha^2}\frac{\partial}{\partial x_\alpha} \tag{12.11c}$$

Now use Eq. (2.178) to find

$$\hat{U}\hat{H}_B\hat{U}^{-1} = \sum_\alpha \left(\frac{\hat{p}_\alpha^2}{2m_\alpha} + \frac{1}{2}m_\alpha\omega_\alpha^2 \left(\hat{x}_\alpha - \sum_n \frac{g_{n\alpha}}{m_\alpha\omega_\alpha^2}|n\rangle\langle n| \right)^2 \right)$$

$$= \hat{H}_B + \frac{1}{2}\sum_n \left(\sum_\alpha \frac{g_{n\alpha}^2}{m_\alpha\omega_\alpha^2} \right)|n\rangle\langle n| - \sum_n \left(\sum_\alpha g_{n\alpha}\hat{x}_\alpha \right)|n\rangle\langle n| \tag{12.12}$$

$$\hat{U}\sum_n \left(E_n + \sum_\alpha g_{n\alpha}\hat{x}_\alpha \right)|n\rangle\langle n|\hat{U}^{-1} = \sum_n \left(E_n + \sum_\alpha g_{n\alpha}\hat{x}_\alpha \right)|n\rangle\langle n|$$

$$- \sum_n \sum_\alpha \frac{g_{n\alpha}^2}{m_\alpha\omega_\alpha^2}|n\rangle\langle n| \tag{12.13}$$

in deriving (12.12) and (12.13) we have used $(|n\rangle\langle n|)^2 = |n\rangle\langle n|$, and the fact that when evaluating transformations such as $\hat{U}\hat{x}_\alpha\hat{U}^{-1}$ the operator $|n\rangle\langle n|$ in $\hat{U}_n$ can be regarded as a scalar. In addition it is easily verified that

$$e^{-i\sum_n |n\rangle\langle n|\hat{\Omega}_n}|n_1\rangle\langle n_2|e^{i\sum_n |n\rangle\langle n|\hat{\Omega}_n} = e^{-i|n_1\rangle\langle n_1|\hat{\Omega}_{n_1}}|n_1\rangle\langle n_2|e^{i|n_2\rangle\langle n_2|\hat{\Omega}_{n_2}}$$

$$= e^{-i\hat{\Omega}_{n_1}}|n_1\rangle\langle n_2|e^{i\hat{\Omega}_{n_2}} = |n_1\rangle\langle n_2|e^{i(\hat{\Omega}_{n_2}-\hat{\Omega}_{n_1})} \tag{12.14}$$

Equations (12.8) and (12.11)–(12.14) yield

$$\hat{\bar{H}} = \sum_n \left(E_n - \left(\sum_\alpha \frac{g_{n\alpha}^2}{2m_\alpha\omega_\alpha^2} \right) \right)|n\rangle\langle n| + \sum_{n\neq n'} V_{n,n'}e^{-i(\hat{\Omega}_n-\hat{\Omega}_{n'})}|n\rangle\langle n'| + \hat{H}_B(\{p_\alpha, x_\alpha\})$$

$$\equiv \hat{\bar{H}}_0 + \sum_{n\neq n'} V_{n,n'}e^{-i(\hat{\Omega}_n-\hat{\Omega}_{n'})}|n\rangle\langle n'| \tag{12.15}$$

In this transformed Hamiltonian $\hat{\bar{H}}_0$ again describes uncoupled system and bath; the new element being a shift in the state energies resulting from the system–bath interactions. In addition, the interstate coupling operator is transformed to

$$\hat{V} = V_{n,n'}|n\rangle\langle n'| \rightarrow \hat{\bar{V}} = V_{n,n'}e^{-i(\hat{\Omega}_n - \hat{\Omega}_{n'})}|n\rangle\langle n'| = V_{n,n'}e^{-\sum_\alpha \lambda_\alpha^{n,n'}(\partial/\partial x_\alpha)}|n\rangle\langle n'|$$
(12.16a)

with

$$\lambda_\alpha^{n,n'} = \lambda_\alpha^{(n)} - \lambda_\alpha^{(n')}; \qquad \lambda_\alpha^{(n)} = \frac{g_{n\alpha}}{m_\alpha\omega_\alpha^2}$$
(12.16b)

To see the significance of this result consider a typical matrix element of this coupling between eigenstates of $\hat{\bar{H}}_0$. These eigenstates may be written as $|n, \mathbf{v}\rangle = |n\rangle\chi_\mathbf{v}(\{x_\alpha\})$, where the elements v_α of the vector $\mathbf{v}$ denote the states of different modes α, that is, $\chi_{n,\mathbf{v}}(\{x_\alpha\}) = \prod_\alpha \chi_{v_\alpha}(x_\alpha)$ are eigenstates of $\hat{H}_B$ and $\chi_{v_\alpha}(x_\alpha)$ is the eigenfunction that corresponds to the v_αth state of the single harmonic mode α. A typical coupling matrix element is then

$$\langle n, \mathbf{v}|\hat{\bar{V}}|n', \mathbf{v}'\rangle = V_{n,n'}\langle\chi_\mathbf{v}(\{x_\alpha\})|e^{-i(\hat{\Omega}_n - \hat{\Omega}_{n'})}|\chi_{\mathbf{v}'}(\{x_\alpha\})\rangle$$
(12.17)

that is, the coupling between two vibronic states $|n, \mathbf{v}\rangle$ and $|n', \mathbf{v}'\rangle$ is given by the bare interstate coupling $V_{n,n'}$ "renormalized" by the term

$$\langle\chi_\mathbf{v}(\{x_\alpha\})|e^{-i(\hat{\Omega}_n - \hat{\Omega}_{n'})}|\chi_{\mathbf{v}'}(\{x_\alpha\})\rangle = \prod_\alpha \langle\chi_{v_\alpha}(x_\alpha)|e^{-\lambda_\alpha^{n,n'}(\partial/\partial x_\alpha)}|\chi_{v_\alpha'}(x_\alpha)\rangle$$

$$= \prod_\alpha \langle\chi_{v_\alpha}(x_\alpha)|\chi_{v_\alpha'}(x_\alpha - \lambda_\alpha^{n,n'})\rangle$$
(12.18)

The absolute square of these term, which depend on $\mathbf{v}$, $\mathbf{v}'$, and the set of shifts $\{\lambda_\alpha^{n,n'}\}$, are known as *Franck–Condon factors*.

12.3.1   The Born Oppenheimer picture

The polaron transformation, executed on the Hamiltonian (12.8)–(12.10) was seen to yield a new Hamiltonian, Eq. (12.15), in which the interstate coupling is "renormalized" or "dressed" by an operator that shifts the position coordinates associated with the boson field. This transformation is well known in the solid-state physics literature, however in much of the chemical literature a similar end is achieved via a different route based on the Born–Oppenheimer (BO) theory of molecular vibronic structure (Section 2.5). In the BO approximation, molecular vibronic states are of the form $\phi_n(\mathbf{r}, \mathbf{R})\chi_{n,\mathbf{v}}(\mathbf{R})$ where $\mathbf{r}$ and $\mathbf{R}$ denote electronic and nuclear coordinates, respectively, $\phi_n(\mathbf{r}, \mathbf{R})$ are eigenfunctions of the electronic Hamiltonian (with corresponding eigenvalues $E_{\text{el}}^{(n)}(\mathbf{R})$) obtained at fixed nuclear coordinates $\mathbf{R}$ and

$\chi_{n,\mathbf{v}}(\mathbf{R})$ are nuclear wavefunctions associated, for each electronic state n, with a nuclear potential surface given by $E_{\text{el}}^{(n)}(\mathbf{R})$. These nuclear potential surfaces are therefore different for different electronic states, and correspond within the harmonic approximation to different sets of normal modes. Mathematically, for any given potential surface, we first find the corresponding equilibrium position, that is, the minimum energy configuration $E_{\text{el,eq}}^{(n)}$, and make the harmonic approximation by disregarding higher than quadratic terms in the Taylor expansion of the potentials about these points. The eigenvectors and eigenvalues of the Hessian matrices of the nth surface, $\mathcal{H}_{\alpha,\alpha'}^{(n)} = (\partial^2 E_{\text{el}}^{(n)}(\mathbf{R})/\partial \mathbf{R}_\alpha \partial \mathbf{R}_{\alpha'})_{\text{eq}}$, yield the normal-mode coordinates, $\mathbf{x}^{(n)} \equiv \{x_\alpha^{(n)}\}$ and the corresponding frequencies $\{\omega_\alpha^{(n)}\}$ of the nuclear motion. In this harmonic approximation the potential surfaces are then

$$E_{\text{el}}^{(n)}(\mathbf{R}) = E_n + \frac{1}{2} \sum_\alpha m_\alpha \omega_\alpha^{(n)2} x_\alpha^{(n)2} \tag{12.19}$$

where $E_n \equiv E_{\text{el,eq}}^{(n)}$.

The sets of normal modes obtained in this way are in principle different for different potential surfaces and can be related to each other by a unitary rotation in the nuclear coordinate space (see further discussion below). An important simplification is often made at this point: We assume that the normal modes associated with the two electronic states are the same, $\{x_\alpha^{(n)}\} = \{x_\alpha\}$, except for a shift in their equilibrium positions. Equation (12.19) is then replaced by

$$E_{\text{el}}^{(n)}(\mathbf{R}) = E_n + \frac{1}{2} \sum_\alpha m_\alpha \omega_\alpha^2 (x_\alpha - \lambda_\alpha^{(n)})^2$$

$$= E_n + \sum_\alpha \hbar \omega_\alpha (\bar{x}_\alpha - \bar{\lambda}_\alpha^{(n)})^2 \tag{12.20}$$

where the dimensionless coordinates and shifts are defined by

$$\bar{x}_\alpha \equiv x_\alpha \sqrt{\frac{m_\alpha \omega_\alpha}{2\hbar}}; \qquad \bar{\lambda}_\alpha^{(n)} \equiv \lambda_\alpha^{(n)} \sqrt{\frac{m_\alpha \omega_\alpha}{2\hbar}} \tag{12.21}$$

A schematic view of the two potential surfaces projected onto a single normal mode is seen in Fig. 12.3. The normal mode shifts $\lambda_\alpha^{(n)}$ express the deviation of the equilibrium configuration of electronic state n from some specified reference configuration (e.g. the ground state equilibrium), projected onto the normal mode directions. Other useful parameters are the single mode reorganization energy E_r^α, defined by the inset to Fig. 12.3,

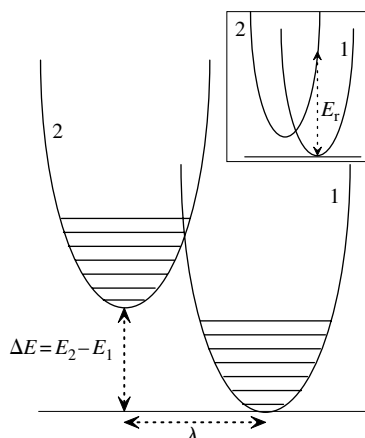$$E_r^\alpha = \hbar \omega_\alpha \bar{\lambda}_\alpha^2 \tag{12.22a}$$

FIG. 12.3 A schematic view of the shifted potential surfaces model, shown for simplicity as a one-dimensional (single mode) representation. The inset is a similar figure on a different scale that shows the reorganization energy E_r.

and the corresponding total reorganization energy

$$E_r = \sum_\alpha E_r^\alpha \tag{12.22b}$$

What is the justification for this approximation? Our accumulated experience in molecular spectroscopy involving low-lying electronic states teaches us that many optical spectra can be interpreted *approximately* using model nuclear potential surfaces in which the *identities* of the normal-mode coordinates do not change in the electronic transition. A geometrical picture of this observation is that the harmonic surfaces shift in parallel with each other. Mixing the normal modes will amount in this picture to a relative rotation of the potential surfaces between the different electronic states, and the assumption is that this rotation is small and may be disregarded to first approximation. Note that this does not mean that the molecular shape remains constant in the transition. Any change in the equilibrium position of a normal mode that is not totally symmetric in the molecular symmetry group will lead to a change in molecular shape.

To summarize, the Born–Oppenheimer states are of the form $\phi_n(\mathbf{r}, \mathbf{R}) \chi_{n,\mathbf{v}}(\mathbf{R})$ where the vibrational wavefunction $\chi_{n,\mathbf{v}}(\mathbf{R})$ is an eigenstate of the nuclear Hamiltonian $\hat{H}_B^{(n)}$ associated with the electronic state n. In the harmonic approximation these Hamiltonians are separable, $\hat{H}_B^{(n)} = \sum_\alpha \hat{h}_{n\alpha}$, so that $\chi_{n,\mathbf{v}}(\mathbf{R}) = \prod_\alpha \chi_{n,v_\alpha}(x_\alpha)$ where χ_{n,v_α} are eigenfunctions of the mode Hamiltonians $\hat{h}_{n\alpha}$. In the shifted harmonic surfaces model these normal modes keep their identity in different electronic states, except that their equilibrium positions depend on the electronic

state. Formally this can be expressed as

$$\hat{h}_{2\alpha} = \hat{U}_\alpha \hat{h}_{1\alpha} \hat{U}_\alpha^{-1} \tag{12.23}$$

where $\hat{U}_\alpha$ is the unitary position shift operator (Eqs (2.173) and (2.175))

$$\hat{U}_\alpha = e^{-\lambda_\alpha (\partial/\partial x_\alpha)} = e^{\bar{\lambda}_\alpha (\hat{a}_\alpha^\dagger - \hat{a}_\alpha)} \tag{12.24}$$

and λ_α is the shift associated with mode α between the two electronic states (same as $\lambda_\alpha^{1,2}$ in the notation of Eq. (12.16)).

   Consider now transition between vibronic levels associated with different electronic states that are described in the Born–Oppenheimer approximation. Any residual coupling $\hat{V}(\mathbf{r}, \mathbf{R})$ not taken into account under the BO approximation, as well as coupling induced by external fields, can cause such transitions. For allowed optical transitions this is the electronic dipole operator. Electronic radiationless relaxation following optical excitation in molecular processes is best described in the full BO picture, whereupon perturbations that lead to interstate coupling between states of the same spin multiplicity stem from corrections to this picture (Eq. (2.53)). Charge transfer processes (Chapter 16) are usually described within a diabatic local state picture, where the dominant interaction is associated with electrons on one center feeling the other. In either case, a general coupling matrix element between two vibronic states $\phi_n(\mathbf{r}, \mathbf{R})\chi_{n,\mathbf{v}}(\mathbf{R})$ and $\phi_{n'}(\mathbf{r}, \mathbf{R})\chi_{n',\mathbf{v}'}(\mathbf{R})$ is of the form

$$V_{n,\mathbf{v};n',\mathbf{v}'} = \langle \chi_{n,\mathbf{v}} | \langle \phi_n | \hat{V}(\mathbf{r}, \mathbf{R}) | \phi_{n'} \rangle_\mathbf{r} | \chi_{n',\mathbf{v}'} \rangle_\mathbf{R} \tag{12.25}$$

where $\langle\rangle_\mathbf{r}$ and $\langle\rangle_\mathbf{R}$ indicate integrations in the electronic and nuclear subspaces, respectively. In the so-called *Condon approximation* the dependence of the electronic matrix element on the nuclear configuration is disregarded, that is, $\langle \phi_n | \hat{V}(\mathbf{r}, \mathbf{R}) | \phi_{n'} \rangle_\mathbf{r} \to V_{n,n'}$ is taken to be independent of $\mathbf{R}$, whereupon

$$V_{n,\mathbf{v};n',\mathbf{v}'} = V_{n,n'} \langle \chi_{n,\mathbf{v}} | \chi_{n',\mathbf{v}'} \rangle_\mathbf{R} \tag{12.26}$$

In the shifted harmonic surfaces model $\chi_{n,\mathbf{v}}(\mathbf{R}) = \prod_\alpha \chi_{n,v_\alpha}(x_\alpha)$ and $\chi_{n',\mathbf{v}'}(\mathbf{R}) = \prod_\alpha \chi_{n',v_\alpha'}(x_\alpha - \lambda_\alpha^{n,n'})$, so Eq. (12.26) is identical to (12.17) and (12.18).

   We have thus found that the interstate coupling (12.17) associated with the Hamiltonian (12.15) is the same as that inferred from the Born–Oppenheimer picture in the Condon approximation, under the assumption that different potential surfaces are mutually related by only rigid vertical and horizontal shifts.[3] In spite

---

[3] Note that the term $\sum_\alpha g_{n\alpha} \hat{x}_\alpha$ in Eq. (12.8) contributes both horizontal and vertical shift: Limiting ourselves to the contribution of a single mode α we have: $E_n + g_\alpha x_\alpha = (1/2)m\omega_\alpha^2 x_\alpha^2 + g_\alpha x_\alpha = (1/2)m\omega_\alpha^2 (x_\alpha - \lambda_\alpha)^2 - (1/2)m\omega_\alpha^2 \lambda_\alpha^2$ where $\lambda_\alpha = g_\alpha/(m\omega_\alpha^2)$. The associated vertical shift is $(1/2)m\omega_\alpha^2 \lambda_\alpha^2 = g_\alpha^2/(2m\omega_\alpha^2)$ which is indeed the vertical shift contribution that enters in Eq. (12.15).

of the approximate nature of the shifted harmonic surfaces picture, this model is very useful both because of its inherent simplicity and because it can be sometimes justified on theoretical grounds as in the electron transfer problem (Chapter 16). The parallel shift parameters λ can be obtained from spectroscopic data or, as again exemplified by the theory of electron transfer, by theoretical considerations.

12.4   Golden-rule transition rates

12.4.1   The decay of an initially prepared level

Let us now return to the two model Hamiltonians introduced in Section 12.2, and drop from now on the subscripts S and SB from the coupling operators. Using the polaron transformation we can describe both models (12.1), (12.2) and (12.4)–(12.6) in a similar language, where the difference enters in the form of the coupling to the boson bath

$$\hat{H} = \hat{H}_0 + \hat{V} \tag{12.27a}$$

$$\hat{H}_0 = E_1|1\rangle\langle1| + E_2|2\rangle\langle2| + \hat{H}_B$$

$$\hat{H}_B = \sum_\alpha \hbar\omega_\alpha \hat{a}_\alpha^\dagger \hat{a}_\alpha \tag{12.27b}$$

In one coupling model we use (12.2b) where, for simplicity, terms with $j = j'$ are disregarded

$$\hat{V} = |1\rangle\langle2| \sum_\alpha V_{1,2}^\alpha (\hat{a}_\alpha^\dagger + \hat{a}_\alpha) + |2\rangle\langle1| \sum_\alpha V_{2,1}^\alpha (\hat{a}_\alpha^\dagger + \hat{a}_\alpha) \tag{12.28a}$$

Sometimes an additional approximation is invoked by disregarding in (12.28a) terms that cannot conserve energy in the lowest order treatment. Under this so-called *rotating wave approximation*[4] the coupling (12.28a) is replaced by (for $E_2 > E_1$)

$$\hat{V}_{\text{RWA}} = |1\rangle\langle2| \sum_\alpha V_{1,2}^\alpha \hat{a}_\alpha^\dagger + |2\rangle\langle1| \sum_\alpha V_{2,1}^\alpha \hat{a}_\alpha \tag{12.28b}$$

---

[4] The rationale for this approximation can be seen in the interaction picture in which $\hat{V}$ becomes

$$\hat{V}_I(t) = \exp((i/\hbar)\hat{H}_0 t)\hat{V}\exp(-(i/\hbar)\hat{H}_0 t)$$

$$= |1\rangle\langle2| \exp((i/\hbar)(E_1 - E_2)t) \sum_\alpha V_{1,2}^\alpha (\hat{a}_\alpha^\dagger \exp(i\omega_\alpha t) + \hat{a}_\alpha \exp(-i\omega_\alpha t)) + h.c.$$

The RWA keeps only terms for which $E_1 - E_2 \pm \hbar\omega_\alpha$ can be small, the argument being that strongly oscillating terms make only a small contribution to the transition rate.

In the other model, Eq. (12.15) written for a two-state system, $\hat{H}_0$ is given again by (12.27b), however now

$$\hat{V} = V_{1,2}e^{i(\hat{\Omega}_2 - \hat{\Omega}_1)}|1\rangle\langle 2| + V_{2,1}e^{-i(\hat{\Omega}_2 - \hat{\Omega}_1)}|2\rangle\langle 1| \qquad (12.29a)$$

$$\hat{\Omega}_2 - \hat{\Omega}_1 = \sum_\alpha \frac{(g_{2\alpha} - g_{1\alpha})\hat{p}_\alpha}{\hbar m_\alpha \omega_\alpha^2} = \sum_\alpha i\bar{\lambda}_\alpha(\hat{a}_\alpha^\dagger - \hat{a}_\alpha) \qquad (12.29b)$$

where we have dropped the tilde notation from the Hamiltonian, denoted $\lambda_{2,1}^\alpha$ simply by λ_α and have redefined the energies E_n to include the shifts $\sum_\alpha g_{n\alpha}^2/(2m_\alpha\omega_\alpha^2)$ that were written explicitly in Eq. (12.15). We have also defined (compare Eq. (2.176))

$$\bar{\lambda}_\alpha \equiv \lambda_\alpha \sqrt{\frac{m_\alpha\omega_\alpha}{2\hbar}} = \frac{g_{2\alpha} - g_{1\alpha}}{m_\alpha\omega_\alpha^2}\sqrt{\frac{m_\alpha\omega_\alpha}{2\hbar}} \qquad (12.30)$$

Equations (12.28) and (12.29) describe different spin-boson models that are commonly used to describe the dynamics of a two-level system interacting with a boson bath. Two comments are in order:

(a) The word "bath" implies here two important attributes of the boson subsystem: First, the boson modes are assumed to constitute a continuum, characterized by a density of modes function $g(\omega)$, so that the number of modes in a frequency range between ω and $\omega + d\omega$ is given by $g(\omega)d\omega$. Second, the boson field is large and relaxes fast relative to the dynamics of the two-level system. It can therefore be assumed to maintain its equilibrium state throughout the process.

(b) The couplings terms (12.28a) and (12.29a) that characterize the two models differ from each other in an essential way: When the spin-boson coupling vanishes ($V_{1,2}^\alpha = 0$ for all α in (2.28); $g_{1\alpha} = g_{2\alpha}$ for all α in (2.29)) the exact system Hamiltonian becomes $\hat{H}_0$ in the first case and $\hat{H}_0 + V$ in the second. The basis states $|1\rangle$ and $|2\rangle$ are therefore eigenstates of the free system in the first case, but can be taken as local states (still coupled by V therefore equivalent to $|L\rangle$ and $|R\rangle$ in Eq. (12.5)) in the second.

As an example consider, within the model (12.29), the time evolution of the system when it starts in a specific state of $\hat{H}_0$, for example, $\Psi(t = 0) = |2, \mathbf{v}\rangle = |2\rangle \prod_\alpha |v_\alpha\rangle$ where $|v_\alpha\rangle$ is an eigenfunctions of the harmonic oscillator Hamiltonian that represents mode α of the boson bath, with the energy $(v_\alpha + (1/2))\hbar\omega_\alpha$. In the absence of coupling to the boson field, namely when $\bar{\lambda}_\alpha = 0$, that is, $\hat{\Omega}_2 - \hat{\Omega}_1 = 0$ in (12.29), the remaining interstate coupling V_{12} cannot change the state $\mathbf{v}$ of the bath and the problem is reduced to the dynamics of two coupled levels ($|2, \mathbf{v}\rangle$ and $|1, \mathbf{v}\rangle$)
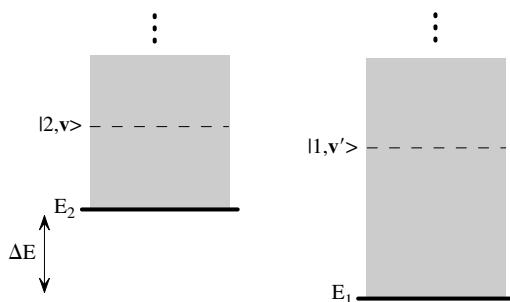
FIG. 12.4 A dressed-states representation of the model of Fig. 12.1.

discussed in Section 2.2, yielding the solution (for $\Psi(t = 0) = |2\rangle$; cf. Eq. (2.32))

$$P_2(t) = 1 - P_1(t)$$

$$P_1(t) = \frac{4|V_{12}|^2}{(E_1 - E_2)^2 + 4|V_{12}|^2} \sin^2\left[\frac{\Omega_R}{2}t\right] \qquad (12.31)$$

where Ω_R is the Rabi frequency, $\Omega_R = (1/\hbar)\sqrt{(E_2 - E_1)^2 + 4|V_{12}|^2}$. Two facts are evident: (1) The specification of the bath state $|\mathbf{v}\rangle$ is immaterial here, and (2) in this case we cannot speak of a *rate* that characterizes the $1 \leftrightarrow 2$ transition.

The coupling to the boson bath can change this in a dramatic way because initial levels of the combined spin–boson system are coupled to a *continuum* of other levels. Indeed Fig. 12.1 can be redrawn in order to display this feature, as seen in Fig. 12.4. Two continuous manifolds of states are seen, "seating" on level 1 and 2, that encompass the states $|1, \mathbf{v}'\rangle = |1\rangle \prod_\alpha |v'_\alpha\rangle$ and $|2, \mathbf{v}\rangle = |2\rangle \prod_\alpha |v_\alpha\rangle$ with zero-order energies $E_{1,\mathbf{v}'}$ and $E_{2,\mathbf{v}}$, respectively, where

$$E_{n,\mathbf{v}} = E_n + E_{\text{boson}}(\mathbf{v}) = E_n + \sum_\alpha \hbar\omega_\alpha(v_\alpha + (1/2)) \qquad (12.32)$$

The continuous nature of these manifolds stems from the continuous distribution of boson modes. The picture is altogether similar to the dressed state picture discussed in Sections 9.2 and 9.3, where states 1 and 2 were ground and excited molecular electronic states, while the boson subsystem was the radiation field, and where we have considered a specific case where level 2 with no photons interacts with the continuum of 1-photon states seating on the ground state 1.

The initial state, $\Psi(t = 0) = |2, \mathbf{v}\rangle = |2\rangle \prod_\alpha |v_\alpha\rangle$, is a state of the overall system—a particular level in the state manifold 2. The general considerations of Section 9.1 (see also Section 10.3.2) have taught us that under certain fairly general conditions the probability to remain in this level decays exponentially by transfer

to states in the manifold 1, with a rate given by the golden-rule formula

$$k_{1 \leftarrow 2\mathbf{v}} = \frac{2\pi}{\hbar} \sum_{\mathbf{v}'} |\langle 2, \mathbf{v}|\hat{V}|1, \mathbf{v}'\rangle|^2 \delta(E_{2,\mathbf{v}} - E_{1,\mathbf{v}'}) \qquad (12.33)$$

The assumption that thermal relaxation in the bath is fast relative to the timescale determined by this rate (see statement (2) of Problem 12.1) makes it possible to define also the thermally averaged rate to go from state 2 to state 1

$$k_{1 \leftarrow 2} = \frac{2\pi}{\hbar} \sum_{\mathbf{v}} P_{\mathbf{v}} \sum_{\mathbf{v}'} |\langle 2, \mathbf{v}|\hat{V}|1, \mathbf{v}'\rangle|^2 \delta(E_{2,\mathbf{v}} - E_{1,\mathbf{v}'}) \qquad (12.34)$$

where (denoting $E_{\mathbf{v}} = E_{\text{boson}}(\mathbf{v})$)

$$P_{\mathbf{v}} = \frac{e^{-\beta E_{2,\mathbf{v}}}}{Q_2} = \frac{e^{-\beta E_{\mathbf{v}}}}{Q_{\text{boson}}}; \qquad \beta = (k_B T)^{-1} \qquad (12.35)$$

$$Q_2 = \sum_{\mathbf{v}} e^{-\beta E_{2,\mathbf{v}}}; \qquad Q_{\text{boson}} = \sum_{\mathbf{v}} e^{-\beta E_{\mathbf{v}}} \qquad (12.36)$$

is the canonical distribution that characterizes the boson bath.

Problem 12.1. Refer to the general discussions of Sections 9.1 and 10.3.2 in order to explain the following two statements: (1) Eq. (12.33) for the partial rates and hence Eq. (12.34) for the thermally averaged rate are valid rate expressions only if the partial rates (12.33) are larger than the inverse of $\hbar \rho_1(E_{2,\mathbf{v}}) = \hbar \sum_{\mathbf{v}'} \delta(E_{2,\mathbf{v}} - E_{1,\mathbf{v}'})$. (2) The thermally averaged rate, $k_{2 \rightarrow 1}$ of Eq. (12.34), is meaningful only if it is much smaller than the rate of thermal relaxation between the levels $\mathbf{v}$ of the initial "2" manifold.

An important observation, made in statement (1) of Problem 12.1, is that we do not really need a continuous distribution of modes in the boson field in order for the manifold (1$\mathbf{v}'$) to be *practically* continuous in the sense that the rate expressions (12.33) and (12.34) are valid. A large finite number, $N \gg 1$, of modes can provide a sufficiently large density of states in manifold 1, $\rho_1(E_{2,\mathbf{v}})$, with energies $E_{1\mathbf{v}'} = \sum_{\alpha=1}^{N} (v_\alpha' + 1/2)\hbar\omega_\alpha$ in the neighborhood of the energy $E_{2,\mathbf{v}}$, provided the energy gap $E_2 - E_1$ is large enough (a reasonable criterion is $E_2 - E_1 \gg \hbar\langle\omega\rangle$ where ω is the average mode frequency). This stems from the huge number of possible combinations of occupation numbers v_α that will yield an energy $E_{1,\mathbf{v}'}$ in a finite neighborhood of any energy $E_{2,\mathbf{v}}$. This is demonstrated by Problem 12.2.

Problem 12.2. Obtain a rough estimate of the density of vibrational states $\rho(E)$ as a function of energy, for a molecule that contains 30 harmonic modes of average frequency $\omega = 500$ cm^{-1} using the following procedure: Assume first that all the modes have the same frequency, 500 cm^{-1}. Then the only possible energy levels (relative to the ground vibrational state) are integer products of this number, $E(L) = 500 \times L$. Calculate the degeneracy $D(L)$ of the energy level $E(L)$ and *estimate* the actual density of states from the results obtained. How fast does $k_{1 \leftarrow 2}$ need to be for an expression like (12.33) to be valid if $E_{21} = 10,000$ cm^{-1}?

Solution: For N modes and $E = \hbar\omega L$ we have L indistinguishable quanta that should be distributed among these N modes. The number of possibilities is a standard problem in combinatorics and the result, $(N + L - 1)!/[(N - 1)!L!]$, is the degeneracy of a level of energy E. The density of states can be roughly estimated to be $\rho(E) = [(N + E/\hbar\omega - 1)!]/[(N - 1)!(E/\hbar\omega)!]/\hbar\omega$. For $\omega = 500$ cm^{-1} and $E = 10\,000$ cm^{-1} this is $49!/(29!20!)/500 \simeq 5.7 \times 10^{10}$ cm, that is, $\rho \sim 5.7 \times 10^{10}$ states per wavenumber or $\sim 2.8 \times 10^{26}$ states per erg. This translates into the time $t = \hbar\rho \sim 0.28$ s. The rate therefore has to be faster than 3.6 s^{-1} for expression (12.33) to hold.

The interstate energy E_{21}, the number of modes N, and the frequency ω used in the estimate made in Problem 12.2 are typical for moderately large molecules. This rationalizes the observation that electronically excited large molecules can relax via *radiationless* pathways in which population is transferred from the excited electronic state to higher vibrational levels of lower electronic states. We may conclude that large isolated molecules can, in a sense, provide their own boson bath and relax accordingly. In such cases, however, the validity of the assumption that thermal relaxation in the boson bath is faster than the $1 \leftrightarrow 2$ transition dynamics may not hold. Radiationless transition rates between electronic states of the same spin multiplicity can be as fast as 10^9–10^{15} s^{-1},[5] while thermal relaxation rates vary. For large molecules in condensed phases thermal equilibrium of nuclear motion is usually achieved within 1–10 ps. For small molecules and for molecules in the gas phase this time can be much longer. In such situations the individual rates (12.33) may have to be considered specifically. We will not consider such cases here.

---

[5] Nonradiative rates that are considerably slower than that will not be observed if the $2 \rightarrow 1$ transition is optically allowed. In the latter case radiative relaxation (i.e. fluorescence) on timescales of 10^{-8}–10^{-9} s will be dominant.

12.4.2 The thermally averaged rate

We now proceed with the thermally averaged $2 \to 1$ rate, Eq. (12.34), rewritten in the form

$$k_{1\leftarrow 2} = \frac{2\pi}{\hbar} \sum_{\mathbf{v}} P_{\mathbf{v}} \sum_{\mathbf{v}'} |\langle \mathbf{v}|\hat{V}_{2,1}|\mathbf{v}'\rangle|^2 \delta(E_2 - E_1 + E_{\text{boson}}(\mathbf{v}) - E_{\text{boson}}(\mathbf{v}'))$$

(12.37)

We will evaluate this rate for the two models considered above. In the model of (12.28a)

$$\hat{V}_{1,2} = \sum_{\alpha} V_{1,2}^{\alpha}(\hat{a}_{\alpha}^{\dagger} + \hat{a}_{\alpha}); \qquad \hat{V}_{2,1} = \sum_{\alpha} V_{2,1}^{\alpha}(\hat{a}_{\alpha}^{\dagger} + \hat{a}_{\alpha}); \qquad V_{2,1}^{\alpha} = (V_{1,2}^{\alpha})^*$$

(12.38)

while from (12.29) in

$$\hat{V}_{1,2} = V_{1,2}e^{-\sum_{\alpha}\bar{\lambda}_{\alpha}(\hat{a}_{\alpha}^{\dagger}-\hat{a}_{\alpha})}; \qquad \hat{V}_{2,1} = V_{2,1}e^{\sum_{\alpha}\bar{\lambda}_{\alpha}(\hat{a}_{\alpha}^{\dagger}-\hat{a}_{\alpha})}; \qquad V_{2,1} = V_{1,2}^*$$

(12.39)

Now use the identity $\delta(x) = (2\pi\hbar)^{-1}\int_{-\infty}^{\infty} dt e^{ixt/\hbar}$ to rewrite Eq. (12.37) in the form

$$k_{1\leftarrow 2} = \frac{1}{\hbar^2}\sum_{\mathbf{v}} P_{\mathbf{v}} \sum_{\mathbf{v}'}\langle \mathbf{v}|\hat{V}_{2,1}|\mathbf{v}'\rangle\langle \mathbf{v}'|\hat{V}_{1,2}|\mathbf{v}\rangle \int_{-\infty}^{\infty} dt e^{i(E_{2\mathbf{v}}-E_{1\mathbf{v}'})t/\hbar}$$

$$= \frac{1}{\hbar^2}\int_{-\infty}^{\infty} dt e^{iE_{2,1}t/\hbar}\sum_{\mathbf{v}} P_{\mathbf{v}}\langle \mathbf{v}|e^{i\hat{H}_B t/\hbar}\hat{V}_{2,1}e^{-i\hat{H}_B t/\hbar}\sum_{\mathbf{v}'}(|\mathbf{v}'\rangle\langle \mathbf{v}'|)\hat{V}_{1,2}|\mathbf{v}\rangle$$

$$= \frac{1}{\hbar^2}\int_{-\infty}^{\infty} dt e^{iE_{2,1}t/\hbar}\langle \hat{V}_{2,1}(t)\hat{V}_{1,2}\rangle$$

(12.40)

where $E_{2,1} = E_2 - E_1$, $\hat{V}_{2,1}(t) = e^{i\hat{H}_B t/\hbar}\hat{V}_{2,1}e^{-i\hat{H}_B t/\hbar}$ is the interaction operator in the Heisenberg representation and where $\langle \cdots \rangle$ denotes a thermal average in the boson subspace. To get this result we have used the fact that $\sum_{\mathbf{v}'}(|\mathbf{v}'\rangle\langle \mathbf{v}'|)$ is a unit operator in the boson subspace.

Problem 12.3. Explain the difference in the forms of Eqs (12.40) and (6.20).

We have thus found that the $k_{1\leftarrow 2}$ is given by a Fourier transform of a quantum time correlation function computed at the energy spacing that characterizes the

two-level system,

$$k_{1 \leftarrow 2} = \frac{1}{\hbar^2} \tilde{C}_{21}(E_{2,1}/\hbar); \qquad \tilde{C}_{21}(\omega) = \int_{-\infty}^{\infty} dt e^{i\omega t} C_{21}(t);$$

(12.41)

$$C_{21}(t) \equiv \langle \hat{V}_{2,1}(t) \hat{V}_{1,2} \rangle$$

Problem 12.4.

(1) Assume that an expression analogous to (12.33) holds also for the transition $|1, \mathbf{v}'\rangle \to 2$, that is,

$$k_{2 \leftarrow 1\mathbf{v}'} = \frac{2\pi}{\hbar} \sum_{\mathbf{v}} |\langle 2, \mathbf{v}|\hat{V}|1, \mathbf{v}'\rangle|^2 \delta(E_{2,\mathbf{v}} - E_{1,\mathbf{v}'})$$

(12.42)

(when would you expect this assumption to be valid?), so that the thermally averaged $1 \to 2$ rate is

$$k_{2 \leftarrow 1} = \frac{2\pi}{\hbar} \sum_{\mathbf{v}'} P_{\mathbf{v}'} \sum_{\mathbf{v}} |\langle 2, \mathbf{v}|\hat{V}|1, \mathbf{v}'\rangle|^2 \delta(E_{2\mathbf{v}} - E_{1,\mathbf{v}'})$$

(12.43)

Using the same procedure as above, show that this leads to

$$k_{2 \leftarrow 1} = \frac{1}{\hbar^2} \int_{-\infty}^{\infty} dt e^{-iE_{2,1}t/\hbar} C_{12}(t); \qquad C_{12}(t) \equiv \langle \hat{V}_{1,2}(t) \hat{V}_{2,1} \rangle \quad (12.44)$$

(2) Use Eqs (12.41), (12.44), and (6.73) to show that

$$k_{2 \leftarrow 1} = k_{1 \leftarrow 2} e^{-E_{2,1}/k_B T}$$

(12.45)

that is, the rates calculated from the golden-rule expression satisfy detailed balance.

12.4.3 Evaluation of rates

For the model (12.28a) $\hat{V}_{1,2}$ and $\hat{V}_{2,1}$ are given by Eq. (12.38) and the corresponding Heisenberg representation operator is $\hat{V}_{j,k}(t) = \sum_{\alpha} V_{j,k}^{\alpha}(\hat{a}_{\alpha}^{\dagger} e^{i\omega_{\alpha} t} + \hat{a}_{\alpha} e^{-i\omega_{\alpha} t})$

where $j = 1, k = 2$ or $j = 2, k = 1$. Using this in (12.41) yields

$$C_{21}(t) = C_{12}(t) = \sum_\alpha |V_{2,1}^\alpha|^2 \langle \hat{a}_\alpha^\dagger \hat{a}_\alpha e^{i\omega_\alpha t} + \hat{a}_\alpha \hat{a}_\alpha^\dagger e^{-i\omega_\alpha t} \rangle$$

$$= \int_0^\infty d\omega g(\omega) |V_{1,2}(\omega)|^2 (n(\omega) e^{i\omega t} + (n(\omega) + 1) e^{-i\omega t}) \quad (12.46)$$

where $n(\omega) = (e^{\beta\hbar\omega} - 1)^{-1}$ is the thermal boson occupation number and $g(\omega) = \sum_\alpha \delta(\omega - \omega_\alpha)$ is the density of modes in the boson field.[6] We note in passing that the function $\sum_\alpha |V_{1,2}^\alpha|^2 \delta(\omega - \omega_\alpha) = g(\omega) |V_{1,2}(\omega)|^2$ is essentially the spectral density, the coupling weighted density of modes (see Sections 6.5.2, 7.5.2, and 8.2.6), associated with the system–bath coupling. We have discussed several models for such functions in Sections 6.5.2 and 8.2.6.

Using Eq. (12.46) in (12.41) we find that for $E_{2,1} > 0$ the term containing $\exp(i\omega t)$ in (12.46) does not contribute to $k_{1\leftarrow 2}$. We get

$$k_{1\leftarrow 2} = \frac{2\pi}{\hbar^2} g(\omega_{2,1}) |V_{1,2}(\omega_{2,1})|^2 (n(\omega_{2,1}) + 1); \qquad \omega_{2,1} = E_{2,1}/\hbar \quad (12.47)$$

Similarly, Eq. (12.44) yields

$$k_{2\leftarrow 1} = \frac{2\pi}{\hbar^2} g(\omega_{2,1}) |V_{1,2}(\omega_{2,1})|^2 n(\omega_{2,1}) \quad (12.48)$$

Note that for a model characterized by an upper cutoff in the boson density of states, for example, the Debye model, these rates vanish when the level spacing of the two-level system exceeds this cutoff. Note also that the rates (12.47) and (12.48) satisfy the detailed balance relationship (12.45).

Next consider the model defined by Eqs (12.27) and (12.29). The correlation functions $C_{21}(t)$ and $C_{12}(t)$ are now

$$C_{21}(t) = \langle \hat{V}_{2,1}(t) \hat{V}_{1,2} \rangle = |V_{2,1}|^2 \prod_\alpha C_{21}^\alpha(t) \quad (12.49a)$$

where

$$C_{21}^\alpha(t) = \langle e^{\bar{\lambda}_\alpha(\hat{a}_\alpha^\dagger e^{i\omega_\alpha t} - \hat{a}_\alpha e^{-i\omega_\alpha t})} e^{-\bar{\lambda}_\alpha(\hat{a}_\alpha^\dagger - \hat{a}_\alpha)} \rangle \quad (12.49b)$$

---

[6] The function $V_{1,2}(\omega)$ is defined by a coarse-graining procedure, $\sum_{\omega_\alpha \in \Delta\omega} |V_{1,2}^\alpha|^2 = \Delta\omega g(\omega) |V_{1,2}(\omega)|^2$ where $\omega_\alpha \in \Delta\omega$ denotes $\omega + \Delta\omega/2 \geq \omega_\alpha \geq \omega - \Delta\omega/2$ and $\Delta\omega$ is large relative to $(g(\omega))^{-1}$. A formal definition is $|V_{12}(\omega)^2| = g^{-1}(\omega) \sum_\alpha |V_{12}^\alpha|^2 \delta(\omega - \omega_\alpha)$.

and

$$C_{12}(t) \equiv \langle \hat{V}_{1,2}(t)\hat{V}_{2,1} \rangle = |V_{2,1}|^2 \prod_\alpha C_{12}^\alpha(t) \tag{12.50a}$$

$$C_{12}^\alpha(t) = \langle e^{-\bar{\lambda}_\alpha(\hat{a}_\alpha^\dagger e^{i\omega_\alpha t} - \hat{a}_\alpha e^{-i\omega_\alpha t})} e^{\bar{\lambda}_\alpha(\hat{a}_\alpha^\dagger - \hat{a}_\alpha)} \rangle \tag{12.50b}$$

These quantum thermal averages over an equilibrium boson field can be evaluated by applying the raising and lowering operator algebra that was introduced in Section 2.9.2.

Problem 12.5. Use the identities

$$e^{\hat{A}}e^{\hat{B}} = e^{\hat{A}+\hat{B}}e^{(1/2)[\hat{A},\hat{B}]} \tag{12.51}$$

(for operators $\hat{A}$, $\hat{B}$ which commute with their commutator $[\hat{A}, \hat{B}]$) and

$$\langle e^{\hat{A}} \rangle_T = e^{(1/2)\langle \hat{A}^2 \rangle_T} \quad \text{(Bloch theorem)} \tag{12.52}$$

(for an operator $\hat{A}$ that is linear in $\hat{a}$ and $\hat{a}^\dagger$) to show that

$$K \equiv \langle e^{\alpha_1\hat{a}+\beta_1\hat{a}^\dagger} e^{\alpha_2\hat{a}+\beta_2\hat{a}^\dagger} \rangle_T = e^{(\alpha_1+\alpha_2)(\beta_1+\beta_2)(n+1/2)+(1/2)(\alpha_1\beta_2-\beta_1\alpha_2)} \tag{12.53}$$

where $n = \langle \hat{a}^\dagger\hat{a} \rangle = (e^{\beta\hbar\omega} - 1)^{-1}$.

Using (12.53) to evaluate (12.49b) and (12.50b) we get

$$C_{21}^\alpha(t) = C_{12}^\alpha(t) = e^{-\bar{\lambda}_\alpha^2(2n_\alpha+1)+\bar{\lambda}_\alpha^2((n_\alpha+1)e^{-i\omega_\alpha t}+n_\alpha e^{i\omega_\alpha t})} \tag{12.54}$$

So that

$$k_{1\leftarrow 2} = k(\omega_{21}); \qquad \omega_{21} = (E_2 - E_1)/\hbar \tag{12.55a}$$

$$k(\omega_{21}) = \frac{|V_{12}|^2}{\hbar^2} e^{-\sum_\alpha \bar{\lambda}_\alpha^2(2n_\alpha+1)} \int_{-\infty}^{\infty} dt\, e^{i\omega_{21}t+\sum_\alpha \bar{\lambda}_\alpha^2(n_\alpha e^{i\omega_\alpha t}+(n_\alpha+1)e^{-i\omega_\alpha t})} \tag{12.55b}$$

Equations (12.55), sometime referred to as multiphonon transition rates for reasons that become clear below, are explicit expressions for the golden-rule transitions rates between two levels coupled to a boson field in the shifted parallel harmonic potential surfaces model. The rates are seen to depend on the level spacing E_{21}, the normal mode spectrum $\{\omega_\alpha\}$, the normal mode shift parameters $\{\bar{\lambda}_\alpha\}$, the temperature (through the boson populations $\{n_\alpha\}$) and the nonadiabatic coupling

parameter $|V_{12}|^2$. More insight on the dependence on these parameters is obtained by considering different limits of this expression.

Problem 12.6. Show that in the limit where both $\bar{\lambda}_\alpha^2$ and $\bar{\lambda}_\alpha^2 n_\alpha$ are much smaller than 1, Eqs (12.55a) and (12.55b) yield the rates (12.47) and (12.48), respectively, where $|V_{1,2}^\alpha|^2$ in Eq (12.46) is identified with $|V_{12}|^2 \bar{\lambda}_\alpha^2$ so that $|V_{12}(\omega)|^2$ in (12.48) is identified with $|V_{12}|^2 \bar{\lambda}^2(\omega)$.

The rate expressions (12.47) and (12.48) are thus seen to be limiting forms of (12.55), obtained in the low-temperature limit provided that $\bar{\lambda}_\alpha^2 \ll 1$ for all α. On the other hand, the rate expression (12.55) is valid if V_{12} is small enough, irrespective of the temperature and the magnitudes of the shifts $\bar{\lambda}_\alpha$.

12.5   Transition between molecular electronic states

Transitions between molecular electronic states are often described by focusing on the two electronic states involved, thus leading to a two-state model. When such transitions are coupled to molecular vibrations, environmental phonons or radiation-field photons the problem becomes a spin–boson-type. The examples discussed below reiterate the methodology described in this chapter in the context of physical applications pertaining to the dynamics of electronic transitions in molecular systems.

12.5.1   The optical absorption lineshape

A direct consequence of the observation that Eqs. (12.55) provide also golden-rule expressions for transition rates between molecular electronic states in the shifted parallel harmonic potential surfaces model, is that the same theory can be applied to the calculation of optical absorption spectra. The electronic absorption lineshape expresses the photon-frequency dependent transition rate from the molecular ground state dressed by a photon, $|\bar{g}\rangle \equiv |g, \hbar\omega\rangle$, to an electronically excited state without a photon, $|x\rangle$. This absorption is broadened by electronic–vibrational coupling, and the resulting spectrum is sometimes referred to as the Franck–Condon envelope of the absorption lineshape. To see how this spectrum is obtained from the present formalism we start from the Hamiltonian (12.7) in which states L and R are replaced by $|\bar{g}\rangle$ and $|x\rangle$ and V_{LR} becomes $V_{\bar{g}x}$—the coupling between molecule and radiation field. The modes $\{\alpha\}$ represent intramolecular as well as intermolecular vibrational motions that couple to the electronic transition

in the way defined by this Hamiltonian,

$$\hat{H} = \left[E_g + \hbar\omega + \sum_\alpha V_g^\alpha(\hat{a}_\alpha^\dagger + \hat{a}_\alpha) \right] |\bar{g}\rangle\langle\bar{g}| + \left[E_x + \sum_\alpha V_x^\alpha(\hat{a}_\alpha^\dagger + \hat{a}_\alpha) \right] |x\rangle\langle x|$$

$$+ V_{\bar{g}x}|\bar{g}\rangle\langle x| + V_{x\bar{g}}|x\rangle\langle\bar{g}| + \sum_\alpha \hbar\omega_\alpha \hat{a}_\alpha^\dagger \hat{a}_\alpha \qquad (12.56)$$

We have already seen that this form of electron–phonon coupling expresses shifts in the vibrational modes equilibrium positions upon electronic transition, a standard model in molecular spectroscopy. Applying the polaron transformation to get a Hamiltonian equivalent to (12.27) and (12.29), then using Eq. (12.34) with $E_2 = E_{\bar{g}} = E_g + \hbar\omega$ and $E_1 = E_x$ leads to the electronic absorption lineshape in the form

$$L_{\text{abs}}(\omega) \sim \sum_{\mathbf{v}} P_{\mathbf{v}} \sum_{\mathbf{v}'} |\langle g\mathbf{v}|\hat{\mu}e^{i(\hat{\Omega}_x - \hat{\Omega}_g)}|x\mathbf{v}'\rangle|^2 \delta(E_g + \hbar\omega - E_x + E_{\text{vib}}(\mathbf{v}) - E_{\text{vib}}(\mathbf{v}'))$$

$$= |\mu_{gx}|^2 \sum_{\mathbf{v}} P_{\mathbf{v}} \sum_{\mathbf{v}'} |\langle\mathbf{v}|e^{i(\hat{\Omega}_x - \hat{\Omega}_g)}|\mathbf{v}'\rangle|^2 \delta(E_g + \hbar\omega - E_x + E_{\text{vib}}(\mathbf{v}) - E_{\text{vib}}(\mathbf{v}'))$$

$$(12.57)$$

where $\hat{\mu}$ is the electronic dipole operator, the molecular–electronic part of the molecule–radiation field coupling, and where in the last expression we have invoked the Condon approximation. As already discussed, the operator $e^{i(\hat{\Omega}_x - \hat{\Omega}_g)}$ affects a rigid displacement of the nuclear wavefunctions. The matrix elements

$$(\text{FC})_{\mathbf{v},\mathbf{v}'} = |\langle\mathbf{v}|e^{i(\hat{\Omega}_x - \hat{\Omega}_g)}|\mathbf{v}'\rangle|^2 \qquad (12.58)$$

called *Franck–Condon factors*, are absolute squares of overlap integrals between nuclear wavefunctions associated with parallel-shifted nuclear potential surfaces.

A word of caution is needed here. The golden-rule expression, Eq. (12.33) or (12.43), was obtained for the rate of decay of a level interacting with a continuous manifold (Section 9.1), not as a perturbation theory result[7] but under certain conditions (in particular a dense manifold of final states) that are not usually satisfied for optical absorption. A similar expression is obtained in the weak coupling limit using time-dependent perturbation theory, in which case other conditions are not

---

[7] This statement should be qualified: The treatment that leads to the golden-rule result for the exponential decay rate of a state interacting with a continuum is not a short-time theory and in this sense nonperturbative, however we do require that the continuum will be "broad." In relaxation involving two-level systems this implies $E_{21} \gg \Gamma = 2\pi V^2 \rho$, that is, a relatively weak coupling.

needed. It is in the latter capacity that we apply it here. The distinction between these applications can be seen already in Eq. (12.33) which, for the zero temperature case (putting $\mathbf{v} = 0$ for the ground vibrational level in the dressed electronic state $|\bar{g}\rangle$), yields

$$k_{x \leftarrow \bar{g}0} = \frac{2\pi}{\hbar} \sum_{\mathbf{v'}} |\langle \bar{g}, 0|\hat{V}|x, \mathbf{v'}\rangle|^2 \delta(E_{\bar{g}0} - E_{x\mathbf{v'}}) \qquad (12.59)$$

This expression can be interpreted as a decay rate of level $|\bar{g}, 0\rangle$ into the manifold $\{|x, \mathbf{v'}\rangle\}$ only if this manifold is (1) continuous or at least dense enough, and (2) satisfies other requirements specified in Section 9.1. Nevertheless, Eq. (12.59) can be used as a lineshape expression even when that manifold is sparse, leading to the zero temperature limit of (12.57)

$$L_{\text{abs}}(\omega) \sim |\mu_{gx}|^2 \sum_{\mathbf{v'}} |\langle 0|e^{i(\hat{\Omega}_x - \hat{\Omega}_g)}|\mathbf{v'}\rangle|^2 \delta(E_g + \hbar\omega - E_x - E_{\text{vib}}(\mathbf{v'})) \quad (12.60)$$

It displays a superposition of lines that correspond to the excitation of different numbers of vibrational quanta during the electronic transition (hence the name multiphonon transition rate). The relative line intensities are determined by the corresponding Franck–Condon factors. The fact that the lines appear as δ functions results from using perturbation theory in the derivation of this expression. In reality each line will be broadened and simplest theory (see Section 9.3) yields a Lorentzian lineshape.

Consider now the $T \to 0$ limit of Eq. (12.55b) written for the absorption lineshape of a diatomic molecule with a single vibrational mode α,

$$L_{\text{abs}}(\omega) \sim |\mu_{gx}|^2 e^{-\bar{\lambda}_\alpha^2} \int_{-\infty}^{\infty} dt e^{-i(\omega_{xg} - \omega)t + \bar{\lambda}_\alpha^2 e^{-i\omega_\alpha t}}$$

$$= |\mu_{gx}|^2 e^{-\bar{\lambda}_\alpha^2} \int_{-\infty}^{\infty} dt e^{-i(\omega_{xg} - \omega)t} \sum_{v=0}^{\infty} \frac{1}{v!} \bar{\lambda}_\alpha^{2v} e^{-iv\omega_a t}$$

$$\sim |\mu_{gx}|^2 \sum_{v=0}^{\infty} \frac{e^{-\bar{\lambda}_\alpha^2}}{v!} \bar{\lambda}_\alpha^{2v} \delta(\omega_{xg} + v\omega_\alpha - \omega) \qquad (12.61)$$

We have seen (Eqs (2.185) and (2.186)) that the coefficients in front of the δ-functions are the corresponding Franck–Condon factors, so Eq. (12.61) is just another way to write Eq. (12.60) with the Franck–Condon factors explicitly evaluated.

Equations (12.60) and (12.61) are expressions for the low temperature (i.e. $k_B T < \hbar \omega_\alpha$) electronic absorption lineshape. The frequency dependence originates from the individual transition peaks, that in reality are broadened by intramolecular and intermolecular interactions and may overlap, and from the Franck–Condon envelope

$$(FC_{0,v}(\omega))_{v=(\omega-\omega_{xg})/\omega_\alpha} = \begin{cases} 0 & \omega < \omega_{xg} \\ e^{-\bar{\lambda}_\alpha^2} \bar{\lambda}_\alpha^{2[(\omega-\omega_{xg})/\omega_\alpha]} / [(\omega - \omega_{xg})/\omega_\alpha]! & \omega > \omega_{xg} \end{cases}$$

(12.62)

This Franck–Condon envelope characterizes the broadening of molecular electronic spectra due to electronic–vibrational coupling.

12.5.2   Electronic relaxation of excited molecules

When a molecule is prepared in an excited electronic state, the subsequent time evolution should eventually take the molecule back to the ground state. This results from the fact that electronic energy spacings ΔE_{el} between lower molecular electronic states are usually much larger than $k_B T$. The corresponding relaxation process may be radiative—caused by the interaction between the molecule and the radiation field and accompanied by photon emission, or nonradiative, resulting from energy transfer from electronic to nuclear degrees of freedom, that is, transition from an excited electronic state to higher vibrational levels associated with a lower electronic state. The excess vibrational energy subsequently dissipates by interaction with the environment (vibrational relaxation, see Chapter 13), leading to dissipation of the initial excess energy as heat.[8] The terms radiative and nonradiative (or radiationless) transitions are used to distinguish between these two relaxation routes. Both processes can be described within the spin–boson model: In the radiative case the radiation field can be represented as a set of harmonic oscillators—the photons, while in the nonradiative case the underlying nuclear motion associated with intramolecular and intermolecular vibrations is most simply modeled by a set of harmonic oscillators.

In what follows we focus on the nonradiative relaxation process (the treatment of radiative relaxation, namely fluorescence, is similar to that of absorption discussed in the previous section). An important observation is that *the mechanism and consequently the rate of the electronic transition depend critically on how the nuclei behave during its occurrence*. Figure 12.5 depicts a schematic view of this process,

---

8   It is also possible that the molecule will dispose of excess vibrational energy radiatively, that is, by infrared emission, however this is not very likely in condensed phases because relaxation to solvent degrees of freedom is usually much faster. Even in low-pressure samples the relaxation due to collisions with the walls is usually more efficient than the infrared emission route.

showing two extreme possibilities for this nuclear motion. In the low-temperature limit route a has to be taken. This is a nuclear tunneling process that accompanies the electronic transition. In the opposite, high-temperature case pathway b dominates. This is an activated process, characterized by an activation energy E_A shown in the figure.

We should keep in mind that the two routes: Tunneling in case a and activation in case b refer to the nuclear motion that underlines the electronic transition. In fact, the mathematical difference between the rates of these routes stems from the corresponding Franck–Condon factors that determine the overlap between the nuclear wavefunctions involved in the transition. The nuclear wavefunctions associated with process a are localized in wells that are relatively far from each other and their mutual overlap in space is small—a typical tunneling situation. In contrast, in process b the electronic transition takes place at the crossing between the nuclear potential surfaces where the overlap between the corresponding nuclear wavefunctions is large. This route will therefore dominate if the temperature is high enough to make this crossing region energetically accessible.

We will see below that the relative importance of these routes depends not only on the temperature but also on the nuclear shift parameters λ, the electronic energy gap ΔE, and the vibrational frequencies. We should also note that these two routes represent extreme cases. Intermediate mechanisms such as thermally activated tunneling also exist. Mixed situations, in which some nuclear degrees of freedom have to be activated and others, characterized by low nuclear masses and small shifts λ, can tunnel, can also take place.

A particular kind of electronic relaxation process is electron transfer. In this case (see Chapter 16) the electronic transition is associated with a large rearrangement of the charge distribution and consequently a pronounced change of the nuclear configuration, which translate into a large λ. Nuclear tunneling in this case is a very low-probability event and room temperature electron transfer is usually treated as an activated process.

12.5.3 The weak coupling limit and the energy gap law

Consider now the application of Eq. (12.55) to the transition rate from an excited electronic state 2 to a lower state 1 in the absence of any external field. For simplicity we focus on the low-temperature limit, $k_B T < \hbar\omega_{\min}$ where $\omega_{\min}$ is the lowest phonon frequency. This implies $n_\alpha = 0$ for all α, so (12.55b) becomes

$$k_{1\leftarrow2}(\omega_{21}) = \frac{|V_{12}|^2}{\hbar^2} e^{-\sum_\alpha \bar{\lambda}_\alpha^2} \int_{-\infty}^{\infty} dt\, e^{i\omega_{21}t + \sum_\alpha \bar{\lambda}_\alpha^2 e^{-i\omega_\alpha t}} \qquad (12.63)$$
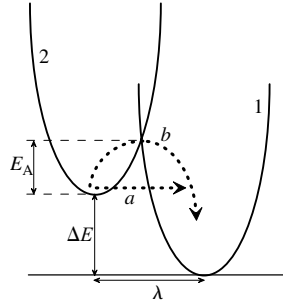
FIG. 12.5 The nuclear tunneling (*a*) and nuclear activation (*b*) pathways to nonradiative electronic relaxation.

where $E_{21} = \hbar\omega_{21}$ has been denoted ΔE in Fig. 12.5. For a single mode model, the analog of Eq. (12.61) is

$$k_{1\leftarrow 2}(\omega_{21}) = \frac{2\pi |V_{12}|^2}{\hbar^2} \sum_{v=0}^{\infty} \frac{e^{-\bar{\lambda}_\alpha^2}}{v!} \bar{\lambda}_\alpha^{2v} \delta(\omega_{21} - v\omega_\alpha)$$

$$\approx \frac{2\pi |V_{12}|^2}{\hbar^2} e^{-\bar{\lambda}_\alpha^2} \frac{\bar{\lambda}_\alpha^{2\bar{v}}}{\bar{v}!}; \qquad \bar{v} = \frac{\omega_{21}}{\omega_\alpha} \tag{12.64}$$

For $\bar{v} \gg 1$, that is, large energy gap, $E_2 - E_1 \gg \hbar\omega_\alpha$, the ω_{21} dependence is given by

$$k_{1\leftarrow 2}(\omega_{21}) \sim \exp(\bar{v} \ln \bar{\lambda}_\alpha^2 - \bar{v} \ln \bar{v}) \tag{12.65}$$

For $\bar{\lambda}_\alpha < 1$ this function decreases exponentially or faster with the energy gap.

The same observation can be made also for the general many-mode case, for which we get

$$k_{1\leftarrow 2}(\omega_{21}) = \frac{2\pi |V_{12}|^2}{\hbar^2} e^{-\sum_\alpha \bar{\lambda}_\alpha^2} \sum_{\{v_\alpha\}} \delta\left(\omega_{21} - \sum_\alpha v_\alpha \omega_\alpha\right) \prod_\alpha \frac{\bar{\lambda}_\alpha^{2v_\alpha}}{v_\alpha!} \tag{12.66}$$

where, as usual, $\{v_\alpha\}$ denotes a set of vibrational quantum numbers, v_α for mode α, that specify a molecular vibrational state. Again we consider the large energy gap limit, $\omega_{21} \gg \omega_c$ where ω_c is the highest phonon frequency. We also focus on the weak electron–phonon coupling limit, $\bar{\lambda}_\alpha^2 \ll 1$ for all modes. In this case the sum in (12.66) is dominated by the terms with the smallest v_α, that is, by modes with $\omega_\alpha \simeq \omega_c$. For an order of magnitude estimate we may replace $\bar{\lambda}_\alpha^2$ for these modes by an average value $\bar{\lambda}^2$, so

$$k_{1\leftarrow 2}(\omega_{21}) \sim \bar{\lambda}^{2(\omega_{21}/\omega_c)} S; \qquad S = \sum_{\substack{\{v_\alpha\} \\ \sum_\alpha v_\alpha = \omega_{21}/\omega_c}} \prod_\alpha \frac{1}{v_\alpha!} \tag{12.67}$$

where the terms that contribute to S are associated with the group of modes with frequencies close to ω_c. Equation (12.67) shows an exponential decrease (since $\bar{\lambda} < 1$) of the rate with increasing $\bar{\nu} \equiv \omega_{21}/\omega_c$, that is, with larger electronic energy gap E_{21}, with corrections that arise from the dependence of S on ω_{21}. $\bar{\nu}$ is the number of vibrational quanta that the n_c high-frequency modes must accept from the electronic motion. If, for example, $n_c \gg \bar{\nu}$, the most important contributions to (12.67) are the $n_c!/\bar{\nu}!$ terms with $\nu_\alpha = 1$ or 0, so that $k_{1\leftarrow 2}(\omega_{21}) \sim \bar{\lambda}^{2\bar{\nu}} n_c!/\bar{\nu}!$ is essentially the same as (12.64) and (12.65).

This "energy gap law": Inverse exponential decrease of the rate on the gap between the electronic origins of the two states involved, characterizes the nuclear tunneling route to electronic relaxation. As discussed above, it stems from the energy gap dependence of the Franck–Condon factors that determine the magnitudes of the dominant contributions to the rate at the given gap. As seen in Section 2.10, tunneling processes depend exponentially on parameters related to the potential barrier. The result obtained here has a similar character but is different in specifics because the electronic energy gap does not reflect a barrier height for the nuclear tunneling process.

12.5.4 The thermal activation/potential-crossing limit

Consider now the opposite case where the shift parameter $\bar{\lambda}^2$ and/or the temperature are large. Specifically we assume $\sum_\alpha \bar{\lambda}_\alpha^2 n_\alpha \gg 1$. In this case the integrand in Eq. (12.55b) is very short-lived and can be approximated by expanding the exponential up to second order in the $\omega_\alpha t$ factors. This short-time approximation leads to

$$k_{1\leftarrow 2} = \frac{|V_{12}|^2}{\hbar^2} e^{-\sum_\alpha \bar{\lambda}_\alpha^2 (2n_\alpha+1)} \int_{-\infty}^{\infty} dt\, e^{i\omega_{21}t + \sum_\alpha \bar{\lambda}_\alpha^2 ((n_\alpha+1)e^{-i\omega_\alpha t} + n_\alpha e^{i\omega_\alpha t})}$$

$$k_{1\leftarrow 2} = \frac{|V_{12}|^2}{\hbar^2} \int_{-\infty}^{\infty} dt\, e^{i\omega_{21}t - it\sum_\alpha \bar{\lambda}_\alpha^2 \omega_\alpha - (1/2)t^2 \sum_\alpha \bar{\lambda}_\alpha^2 \omega_\alpha^2 (2n_\alpha+1)}$$

$$= \frac{|V_{12}|^2}{\hbar^2} \sqrt{\frac{\pi}{a}} e^{-(\omega_{21}-E_r/\hbar)^2/4a}; \qquad a = \frac{1}{2}\sum_\alpha (2n_\alpha + 1)\bar{\lambda}_\alpha^2 \omega_\alpha^2 \quad (12.68)$$

where E_r is the reorganization energy defined by Eqs. (12.22). A simpler equation is obtained in the classical limit where $n_\alpha = k_B T/\hbar\omega_\alpha$ for all modes α, so $a = k_B T E_r/\hbar^2$:

$$k_{1\leftarrow 2} = \frac{|V_{12}|^2}{\hbar} \sqrt{\frac{\pi}{k_B T E_r}} e^{-(E_{21}-E_r)^2/4k_B T E_r} \qquad (12.69)$$

This result has the form of a thermally activated rate, with activation energy given by

$$E_A = \frac{(E_{21} - E_r)^2}{4E_r} \tag{12.70}$$

Problem 12.7. Show that E_A, Eq. (12.70) is equal to the height of the *minimum-energy crossing point* of the two potential surfaces $E_{el}^{(1)}(\mathbf{R})$ and $E_{el}^{(2)}(\mathbf{R})$ (Eq. (12.20)) above the bottom of the $E_{el}^{(2)}(\mathbf{R})$ potential surface.

Solution: The two N-dimensional potential surfaces (N—number of phonon modes) cross on an $(N - 1)$—dimensional surface defined by $E_{el}^{(1)}(\{x_\alpha\}) = E_{el}^{(2)}(\{x_\alpha\})$ where $E_{el}^{(1)}(\{x_\alpha\}) = \sum_\alpha \hbar\omega_\alpha (\bar{x}_\alpha - \bar{\lambda}_\alpha)^2 - E_{21}$ and $E_{el}^{(2)}(\{x_\alpha\}) = \sum_\alpha \hbar\omega_\alpha \bar{x}_\alpha^2$. Using Eq. (12.22) the equation for this surface is

$$-2\sum_\alpha \hbar\omega_\alpha \bar{x}_\alpha \bar{\lambda}_\alpha + E_r - E_{21} = 0 \tag{12.71}$$

The crossing point of minimum energy can be found as the minimum of $E_{el}^{(2)}(\{x_\alpha\})$ under the condition (12.71). Defining the Lagrangian $F = \sum_\alpha \hbar\omega_\alpha \bar{x}_\alpha^2 + B(-2\sum_\alpha \hbar\omega_\alpha \bar{x}_\alpha \bar{\lambda}_\alpha + E_r - E_{21})$ the condition for extremum is found as $\bar{x}_\alpha = B\bar{\lambda}_\alpha$. Using this in (12.71) yields the Lagrange multiplier $B = -(E_{21} - E_r)/2E_r$, whence

$$x_\alpha^{(\min)} = -\frac{(E_{21} - E_r)\lambda_\alpha}{2E_r} \tag{12.72}$$

The energy at the lowest energy crossing point is $E_A = E_{el}^{(2)}(\{x_\alpha^{\min}\})$. Using (12.72) and (12.22) leads indeed to (12.70).

We have thus found that in this high temperature, strong electron–phonon coupling limit the electronic transition is dominated by the lowest crossing point of the two potential surfaces, that is, the system chooses this pathway for the electronic transition. It is remarkable that this result, with a strong characteristic of classical rate theory, was obtained as a limiting form of the quantum golden-rule expression for the transition rate. Equation (12.69) was first derived by Marcus in the context of electron transfer theory (Chapter 16).

12.5.5 Spin–lattice relaxation

The evaluation of relaxation rates in the previous sections was based on the assumption that the energy spacing in the two-level system under consideration is large
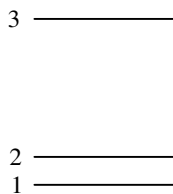
3 ⎯⎯⎯⎯⎯

2 ⎯⎯⎯⎯⎯
1 ⎯⎯⎯⎯⎯

FIG. 12.6 A three-level system used in the text to demonstrate the promotion of effective coupling between spin levels 1 and 2 via their mutual coupling with level 3.

relative to the maximum (cutoff) phonon frequency. This is the common state of affairs for nonradiative electronic relaxation processes, resulting in the multiphonon character of these processes. When the two-level energy spacing is smaller than the boson cutoff frequency, the relaxation is dominated by one-boson processes and may be studied with the Hamiltonian (12.27) and (12.28). Radiative relaxation associated with the interaction (12.3) is an example. The rates associated with such one-boson relaxation processes are given by Eqs (12.47) and (12.48).[9] They are proportional to $g(\omega_{21})$, the boson mode density at the two-level frequency. In the high-temperature limit, $k_B T \gg E_{21}$, they are also proportional to T.

Consider now the case where the energy spacing E_{21} is very small. Such cases are encountered in the study of relaxation between spin levels of atomic ions embedded in crystal environments, so called *spin–lattice relaxation*. The spin level degeneracy is lifted by the local crystal field and relaxation between the split levels, caused by coupling to crystal acoustical phonons, can be monitored. The relaxation as obtained from (12.47) and (12.48) is very slow because the density of phonon modes at the small frequency ω_{21} is small (recall that $g(\omega) \sim \omega^2$).

In fact, when $\omega_{21} \to 0$, other relaxation mechanisms should be considered. It is possible, for example, that the transition from level 2 to 1 is better routed through a third, higher-energy level, 3, as depicted in Fig. 12.6, because the transition rates $k_{3\leftarrow2}$ and $k_{1\leftarrow3}$ are faster than $k_{1\leftarrow2}$. In this case, sometimes referred to as the *Orbach mechanism*, the transition $2 \to 3$ is the rate-determining step and, if $k_B T \ll E_{32}$, the observed relaxation will depend exponentially on temperature, $k_{1\leftarrow2,\text{apparent}} = \exp(-E_{32}/k_B T)$. Another relaxation mechanism is a two-phonon process analogous to Raman light scattering. We note that the one-phonon coupling (12.2b) is a first-order term in an expansion in bath normal mode coordinate. The second-order term in this expansion leads to interaction terms such as

$$\hat{V}_{\text{SB}} = \sum_{\alpha,\beta} (V_{1,2}^{\alpha,\beta}|1\rangle\langle2| + V_{2,1}^{\alpha,\beta}|2\rangle\langle1|)(\hat{a}_\alpha^\dagger + \hat{a}_\alpha)(\hat{a}_\beta^\dagger + \hat{a}_\beta) \qquad (12.73)$$

---

[9] The measured relaxation rate in a process $A \overset{k_1}{\underset{k_2}{\leftrightarrows}} B$ is $k_1 + k_2$.

According to Eq. (12.40) the golden-rule rate is now given by

$$k_{1\leftarrow 2} = \frac{1}{\hbar^2} \sum_{\alpha,\beta} |V_{1,2}^{\alpha,\beta}|^2 \int_{-\infty}^{\infty} dt e^{i\omega_{21}t} \langle (\hat{a}_\alpha^\dagger e^{i\omega_\alpha t} + \hat{a}_\alpha e^{-i\omega_\alpha t})(\hat{a}_\beta^\dagger e^{i\omega_\beta t} + \hat{a}_\beta e^{-i\omega_\beta t})$$

$$\times (\hat{a}_\alpha^\dagger + \hat{a}_\alpha)(\hat{a}_\beta^\dagger + \hat{a}_\beta) \rangle \qquad (12.74)$$

Only terms with $\alpha \neq \beta$ that satisfy $\omega_\alpha - \omega_\beta = \pm\omega_{21}$ survive the time integration. We get

$$k_{1\leftarrow 2} = \frac{2\pi}{\hbar^2} \sum_{\alpha,\beta} |V_{1,2}^{\alpha,\beta}|^2 (\langle \hat{a}_\alpha^\dagger \hat{a}_\beta \hat{a}_\alpha \hat{a}_\beta^\dagger \rangle \delta(\omega_{21} + \omega_\alpha - \omega_\beta)$$

$$+ \langle \hat{a}_\alpha \hat{a}_\beta^\dagger \hat{a}_\alpha^\dagger \hat{a}_\beta \rangle \delta(\omega_{21} - \omega_\alpha + \omega_\beta))$$

$$= \frac{2\pi}{\hbar^2} \sum_{\alpha,\beta} |V_{1,2}^{\alpha,\beta}|^2 [n(\omega_\alpha)(n(\omega_\beta) + 1)\delta(\omega_{21} + \omega_\alpha - \omega_\beta)$$

$$+ (n(\omega_\alpha) + 1)n(\omega_\beta)\delta(\omega_{21} - \omega_\alpha + \omega_\beta)]$$

$$\simeq \frac{4\pi}{\hbar^2} \int_0^{\omega_D} d\omega g^2(\omega)|V_{1,2}(\omega)|^2 n(\omega)(n(\omega) + 1) \qquad (12.75)$$

where $n(\omega) = (e^{\hbar\omega/k_B T} - 1)^{-1}$, ω_D is the Debye frequency and where in the last step we have converted the double sum to a double integral over the normal modes, have used the δ functions to do one integration and have approximated the resulting integrand by taking the limit $\omega_{21} \to 0$. We have also assumed for simplicity that $|V_{1,2}^{\alpha,\beta}|^2$ depends on α and β only through $\omega_\alpha \simeq \omega_\beta$.

   Further analysis is possible only if more information on $V_{1,2}(\omega)$ is available. The theory of spin lattice relaxation leads to $V_{1,2}(\omega) \sim \omega$. At low temperature the integral in (12.75) is dominated by the low-frequency regime where we can use $g(\omega) \sim \omega^2$ (see Section 4.2.4). We then have

$$k_{1\leftarrow 2} \sim \int_0^{\omega_D} d\omega \omega^6 n(\omega)(n(\omega) + 1) \qquad (12.76)$$

and provided that $T \ll \hbar\omega_D/k_B$ this leads to (compare to the analysis of the low-temperature behavior of Eq. (4.52))

$$k_{1\leftarrow 2} \sim T^7 \qquad (12.77)$$

Indeed, both the exponential temperature dependence that characterize the Orbach process and the T^7 behavior associated with the Raman type process have been observed in spin lattice relaxation.[10]

12.6   Beyond the golden rule

The golden-rule rate expressions obtained and discussed above are very useful for many processes that involve transitions between individual levels coupled to boson fields, however there are important problems whose proper description requires going beyond this simple but powerful treatment. For example, an important attribute of this formalism is that it focuses on the rate of a given process rather than on its full time evolution. Consequently, a prerequisite for the success of this approach is that the process will indeed be dominated by a single rate. In the model of Figure 12.3, after the molecule is excited to a higher vibrational level of the electronic state 2 the relaxation back into electronic state 1 is characterized by the single rate (12.34) only provided that thermal relaxation within the vibrational subspace in electronic state 2 is faster than the $2 \rightarrow 1$ electronic transition. This is often the case in condensed phase environments but exceptions have been found increasingly often since picosecond and femtosecond timescales became experimentally accessible. Generalized golden-rule approaches may still be useful in such cases.[11]

In many cases, reliable theoretical descriptions of multi-rate processes can be obtained by using master equations in which individual rates are obtained from golden-rule type calculations (see Sections 8.3.3 and 10.4). A condition for the validity of such an approach is that individual rate processes will proceed independently. For example, after evaluating the rates $k_{1\leftarrow 2}$ and $k_{2\leftarrow 1}$, Eqs (12.55a) and (12.55b), a description of the overall dynamics of the coupled two-level system by the kinetic scheme $1 \underset{k_{1\leftarrow 2}}{\overset{k_{2\leftarrow 1}}{\rightleftarrows}} 2$ relies on the assumption that after each transition, say from 1 to 2, the system spends a long enough time in state 2, become equilibrated in this state (or, more poetically, forgets its past), so that the reverse transition occurs independently. When this is not the case such simple kinetic schemes fail. Generalized quantum master equations (e.g. Section 10.4.2) can be used in such cases, however they are often hard to implement. Note that situations in which successive processes are not decoupled from each other occur also in classical systems.

---

[10]   P. L. Scott and C. D. Jeffries, Phys. Rev. **127**, 32 (1962); G. H. Larson and C. D. Jeffries, Phys. Rev. **141**, 461 (1966).

[11]   R. D. Coalson, D. G. Evans, and A. Nitzan, J. Chem. Phys. **101**, 436 (1994); M. Cho and R. J. Silbey, J. Chem. Phys. **103**, 595 (1995).

Other cases that require going beyond the golden-rule involve transitions which by their nature are of high order in the interaction. Processes studied in conjunction with nonlinear spectroscopy (see Section 18.7) are obvious examples.

Finally, the golden-rule fails when the basic conditions for its validity are not satisfied. For a general review of these issues see Leggett et al.[12] Conditions for the validity of the golden-rule involve relatively uniform coupling to a relatively wide continuum, and one consistency check is that the decaying level, broadened by the decay width Γ, is still wholly contained within the continuum. For example, referring to Fig. 12.4, this is not satisfied for a level near the origin of state 2 if $\Gamma = 2\pi V^2 \rho > \Delta E$. Such "overdamped" cases have to be handled by more advanced methodologies, for example, path integral methods[13] that are beyond the scope of this text.

---

[12] A. J. Leggett, S. Chakravarty, A. T. Dorsey, M. P. A. Fisher, A. Garg, and W. Zwerger, Rev. Mod. Phys. **59**, 1 (1987).

[13] N. Makri and D. E. Makarov, J. Chem. Phys. **102**, 4600 (1995); **102**, 4611 (1995); D. G. Evans, A. Nitzan, and M. A. Ratner, J. Chem. Phys. **108**, 6387 (1998).